2-D Modelling of the JET Divertor

R Simonini, G Corrigan, J Spence, A Taroni, G Vlases.

JET Joint Undertaking, Abingdon, Oxon, OX14 3EA.

2-D MODELLING OF THE JET DIVERTOR

R Simonini, G Corrigan, J Spence, A Taroni, G Vlases
JET Joint Undertaking, Abingdon, OX14 3EA , U.K.

1. Introduction

The design of the first version (Mk I) of the JET pumped divertor is fixed, but various "advanced" geometries are being studied for the second phase (Mk II).

The two main characteristics that determine a good divertor are the divertor's ability to handle power exhaust at acceptable erosion rates and its control of the impurity production and retention in the scrape-off layer (SOL). A high recycling regime is favourable for both aspects.

For modelling studies, the JET code EDGE2D [1] has been updated (EDGE2D/U). The new code treats impurities self-consistently and allows for targets with an arbitrary inclination with respect to the magnetic field lines. We have carried out studies of divertor performance using EDGE2D/U for different geometrical configurations, showing that the geometry of the divertor chamber plays an essential role, because i) it controls the accessibility to the high recycling regime by influencing the return of neutrals to the main plasma, and ii) it can increase the wetted area on targets, thus reducing peak heat load.

2. A Summary of the Model

In EDGE2D/U, fluid equations for the conservation of particles, momentum and energy are solved for hydrogenic and impurity ions. The electron density is evaluated from quasi-neutrality. The model allows for arbitrarily high impurity concentrations, with the full non-coronal distribution of impurity charge states and the corresponding energy losses being determined. A single impurity temperature, set equal to the hydrogen ion temperature, is assumed. Particle and energy sources due to neutrals recycled and sputtered at the target and chamber walls are computed by a full 2D Monte Carlo module (NIMBUS).

The metric coefficients needed for the transport equations are computed from a two-dimensional mesh derived from the magnetic flux surfaces obtained from MHD computation of JET equilibria, taking the material wall into consideration.

In the calculations reported here we have assumed full plasma recycling at the divertor targets, but other schemes have also been considered. Constant transport coefficients across magnetic surfaces have been used. Matching of experimental decay lengths at the midplane for JET [2] has suggested the choice $\chi_i = \chi_e = 2.0 m^2 s^{-1}$, $D_\perp = 0.1 m^2 s^{-1}$, increased by a factor of five in the divertor region. No inward pinch has been considered so far. We have assumed the input power $P_i = P_e = 10 MW$. The wall material is Carbon.

3. Comparison of results for two divertor configurations

We have continued studies of several divertor geometries for which preliminary results were reported in [3]. Here we report only the results for two of them, since they represent the extreme cases. The first is the Mk I configuration currently being installed at JET. The

second one could be achieved in a Second Phase of the JET divertor operations; namely, a baffled vertical plate design where recycling neutrals are directed more toward the private region (Mk II). The two configurations are sketched in Fig. 1 and 2, where "S", "1" and "2" refer to separatrix and flux surfaces 1 and 2 cm beyond separatrix at the midplane.

The possibility of reaching high density and low temperature regimes has been studied by means of a scan of the density at the separatrix from 1 to 2 $\times 10^{19} m^{-3}$, which is expected to be reached in JET at the power level considered. A summary of relevant results is given the the following table. Here n_S is the density at the separatrix on the outer midplane ($\times 10^{19} m^{-3}$), n_T is the density at the outer strike point, Te_S is the electron temperature at the separatrix on the outer midplane (eV), Te_T is the electron temperature at the outer strike point, P_H is the power loss due to the atomic processes of charge exchange and ionization (with its associated radiation loss) of the hydrogen (MW), P_R is the radiation from impurities, $R_H^{SOL/T}$ is the ratio of the hydrogen source in the SOL to that in the SOL plus divertor, $R_Z^{SOL/T}$ is the corresponding ratio for Carbon, S_Z is the total source of impurities ($\times 10^{21} m^{-3} s^{-1}$), $n_{Z,S}$ is the Carbon density at the separatrix on the outer midplane ($\times 10^{17} m^{-3}$).

Mk	n_S	n_T	Te_S	Te_T	P_H	P_R	$R_H^{SOL/T}$	$R_Z^{SOL/T}$	S_Z	$n_{Z,S}$
I	1	1.3	123	116	3.7	0.2	23%	18%	3.1	0.6
	1.6	7.6	77	29	6.4	1.9	13%	6.1%	5.1	3.8
	2	16	75	15	8.3	2.7	12%	4.8%	3.2	2.3
II	1	20	81	6	9.1	1.1	0.5%	0.5%	4.3	2.4
	1.6	35	79	1.3	11	1.8	0.4%	0.1%	3.3	2.7
	2	47	77	0.6	14	1.6	0.2%	0.3%	1.9	1.4

The principal effect of changing the geometrical configuration is to affect the distribution of ionisation sources due to plasma recycling. This in turn affects the profiles of temperature, density and flow. Mk II is more closed to neutrals than Mk I, as shown by the much smaller relative sources in the SOL $R_H^{SOL/T}$ and $R_Z^{SOL/T}$. Higher target densities and lower temperature are obtained in Mk II than in Mk I for all values of n_S. Thus the total impurity production is also lower except at very low density. Impurities are better retained in Mk II. The power load due to conduction and convection to the targets is lower in Mk II than in Mk I, not only because the wetted area is larger (Figs. 1,2), but also because the total radiation loss is larger (see Table). This is illustrated in Fig 3 for the low-density case $n_S \simeq 10^{19} m^{-3}$ which is the most severe case. The near-orthogonal case Mk I has a relatively peaked distribution which requires sweeping to reduce loads to an acceptable level, while the vertical geometry Mk II can be operated without sweeping. Mk II shows an inversion of the temperature profile at the target, the temperature being lower at the separatrix (Fig.4). This effect is due to the vertical targets that push neutrals toward the separatrix, thus increasing the ionisation source there. The effect is overall beneficial because the high temperature on the chamber side ($\simeq 20eV$) is compensated by the very low density ($\simeq 10^{17} m^{-3}$), thus limiting

sputtering to acceptable levels. In Mk I, instead, the temperature is higher where the density is higher. As the density n_S increases to $2 \times 10^{19} m^{-3}$, in the case of Mk II the plasma enters a regime of very low temperature and high density at the target, and the production of impurities is reduced (Fig.5 and Table). In this regime the power conducted and convected to the plates is only 20% of the input power. Of course, the power to the target should also include the recombination energy and some fraction of the divertor radiated power. The performance of Mk I also improves with n_S as expected, but at a lower rate than Mk II (Fig.5 and Table for $n_S \simeq 2 \times 10^{19} m^{-3}$). It is worthwhile to note that, while the decay lenghts of T_e and T_i in the SOL at the midplane are relatively insensitive to n_S and to the geometrical configuration, the decay length of the density depends on both (for a given power input). This is illustrated in Fig.6, which shows the radial density profiles at the outer midplane for various cases. The density profiles actually depend on the ratio of the perpendicular and parallel transport of particles. However, the parallel transport depends on the flow velocity $v_{\parallel}$ which in turn depends strongly on the distribution of sources and on the temperature at the targets, under the assumption that $v_{\parallel} = v_{sound}$ at the targets. This result should be tested experimentally and may modify results of predictions based on simpler models. As far as impurity radiation P_R is concerned, we have found that in all of the configurations considered P_R is less that 15% of the total input power if sputtered carbon is considered. P_R is marginally larger in Mk I than MK II because more impurities are sputtered in MK I. The situation is opposite at low density. Studies of increasing impurity radiation by injecting impurities at some distance from the target are being carried out at present.

4. Conclusions

Geometrical effects in the divertor can affect significantly the plasma density and temperature profiles, the radiation pattern and the distribution of heat loading on the targets. These effects on the density profile may be important even at the midplane, if n_S is large enough. In general, a closed divertor such as Mk II is more effective than the open Mk I in alleviating the heat load on the targets, thus reducing or eliminating the need of sweeping, and in retaining impurities. Total atomic losses (mainly from hydrogen) can amount to a large fraction of the input power for Mk II, and increase rapidly with density. The wall material seems to be relatively unimportant since most of the radiation comes from the hydrogen. It is expected that geometry effects would play less of a role at higher densities than those considered here, but such conditions might not be attainable in JET.

5. References

[1] A Taroni et al, Proc. 3rd Plasma Edge Theory Meeting, Bad Honnef, Germany (June 1992), to appear in Contributions to Plasma Physics.

[2] R Simonini et al, Journal of Nuclear Materials Vols. 196-198 (1992)369

[3] The JET Team, Proc. 14th Conf. on Plasma Phys. and Contr. Therm. Fus., IAEA Paper CN-56/A-5-1, Wuerzburg Oct 1992

FIG. 1

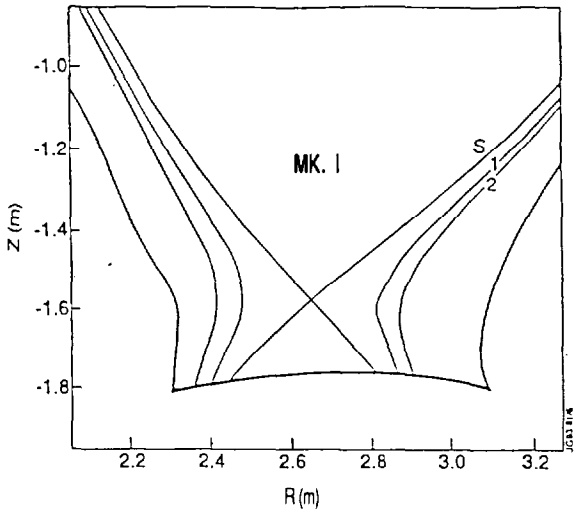

FIG.2

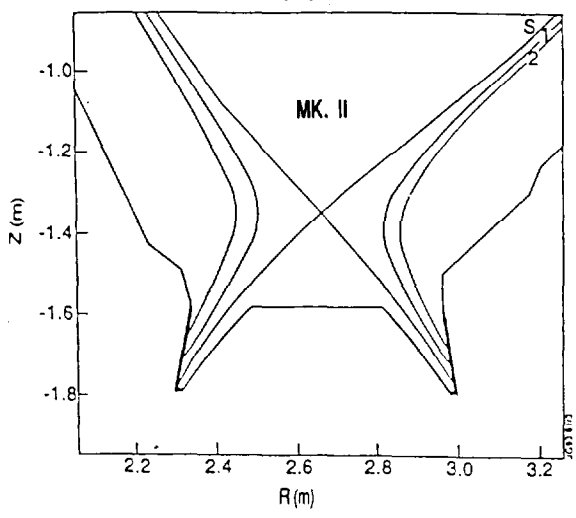

FIG. 3

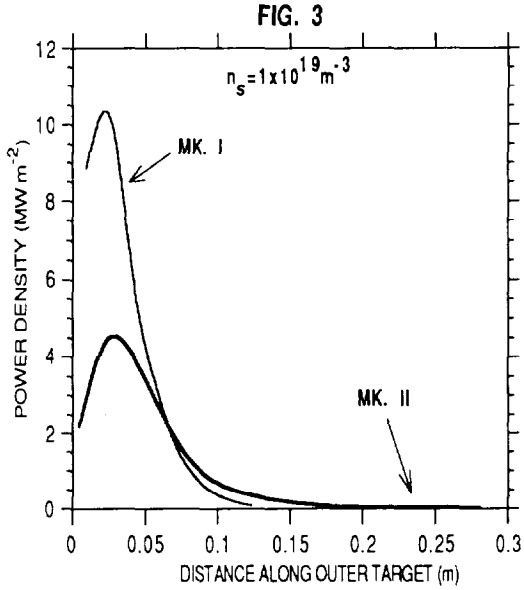

FIG. 4

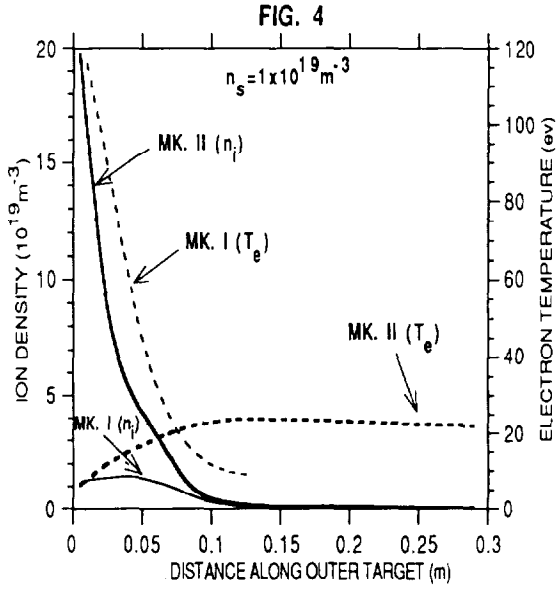

FIG. 5

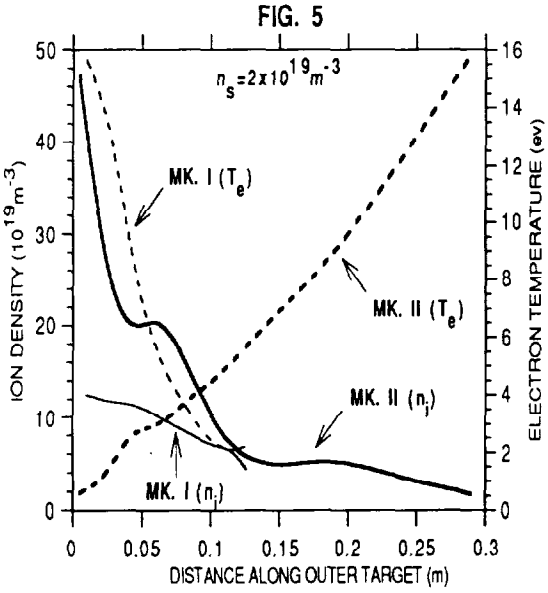

FIG. 6